Acta Biomaterialia 46 (2016) 211–220

Contents lists available at ScienceDirect

Acta Biomaterialia

journal homepage: www.elsevier.com/locate/actabiomat

Full length article

Biodegradable functional polycarbonate micelles for controlled release of amphotericin B

Ying Wang [a,1], Xiyu Ke [b,1], Zhi Xiang Voo [b], Serene Si Ling Yap [a], Chuan Yang [b], Shujun Gao [b], Shaoqiong Liu [b], Shrinivas Venkataraman [b], Sybil Akua Okyerewa Obuobi [a], Jasmeet Singh Khara [a], Yi Yan Yang [b,*], Pui Lai Rachel Ee [a,*]

[a] Department of Pharmacy, National University of Singapore, 18 Science Drive 4, Singapore 117543, Singapore
[b] Institute of Bioengineering and Nanotechnology, 31 Biopolis Way, Singapore 138669, Singapore

ARTICLE INFO

Article history:
Received 12 July 2016
Received in revised form 31 August 2016
Accepted 25 September 2016
Available online 26 September 2016

Keywords:
Polymeric micelles
Amphotericin B
Phenylboronic acid
Polycarbonate
Systemic fungal infection

ABSTRACT

Amphotericin B (AmB), a poorly soluble and toxic antifungal drug, was encapsulated into polymeric micelles self-assembled from phenylboronic acid-functionalized polycarbonate/PEG (PEG-PBC) and urea-functionalized polycarbonate/PEG (PEG-PUC) diblock copolymers *via* hydrogen-bonding, boronate ester bond, and/or ionic interactions between the boronic acid group in the micellar core and amine group in AmB. Three micellar formulations were prepared: AmB/B micelles using PEG-PBC, AmB/U micelles using PEG-PUC and AmB/B+U mixed micelles using 1:1 molar ratio of PEG-PBC and PEG-PUC. The average particle sizes of the micelles were in the range of 54.4–84.8 nm with narrow size distribution and zeta potentials close to neutral. UV–Vis absorption analysis indicated that AmB/B micelles significantly reduced AmB aggregation status due to the interactions between AmB and the micellar core, while Fungizone® and AmB/U micelles had no effect. AmB/B+U mixed micelles exerted an intermediate effect. Both AmB/B micelles and AmB/B+U mixed micelles showed sustained drug release, with 48.6 ± 2.1% and 59.2 ± 1.8% AmB released respectively after 24 h under sink conditions, while AmB/U micelles displayed a burst release profile. All AmB-loaded micelles showed comparable antifungal activity to free AmB or Fungizone®, while AmB/B micelles and AmB/B+U mixed micelles were much less hemolytic than other formulations. Histological examination showed that AmB/B and AmB/B+U micelles led to a significantly lower number of apoptotic cells in the kidneys compared to Fungizone®, suggesting reduced nephrotoxicity of the micellar formulations *in vivo*. These phenylboronic acid-functionalized polymeric micelle systems are promising drug carriers for AmB to reduce non-specific toxicities without compromise in antifungal activity.

Statement of Significance

There is a pressing need for a novel and cost-effective delivery system to reduce the toxicity induced by the antifungal agent, amphotericin B (AmB). In this study, phenylboronic acid-functionalized polycarbonate/PEG diblock copolymers were used to fabricate micelles for improved AmB-micelle interaction via the manipulation of hydrogen-bonding, boronate ester bond, ionic and hydrophobic interactions. Compared to free AmB and Fungizone®, the resultant micellar systems displayed improved stability while reducing non-specific toxicities without a compromise in antifungal activity. These findings demonstrate the potential of biodegradable functional polycarbonate micellar systems as promising carriers of AmB for the treatment of systemic fungal infections.

1. Introduction

Systemic fungal infections are posing a global health concern due to the significant morbidity and mortality in immunocompromised patients [1]. The polyene macrolide antibiotic amphotericin B (AmB) exhibits a broad-spectrum antifungal activity and is a crucial therapeutic option for the treatment of severe systemic mycosis [2]. However, the life-saving benefits of AmB are impaired by its toxicities to normal tissues, which induce various side effects, including infusion-related toxicity and chronic toxicities, such as nephrotoxicity, cardiotoxicity, hepatoxicity, leukopenia and thrombocytopenia [3]. The toxicities of AmB are associated with

* Corresponding authors.
E-mail addresses: yyyang@ibn.a-star.edu.sg (Y.Y. Yang), phaeplr@nus.edu.sg (P.L.R. Ee).
[1] These authors contributed equally to this work.

http://dx.doi.org/10.1016/j.actbio.2016.09.036
1742-7061/

the formation of soluble aggregates due to its amphoteric nature. The selectivity of AmB between fungal and mammalian cells depends on the aggregation state of AmB and the nature of membrane sterol. Monomeric AmB is the only form present at low AmB concentration, while the aggregated form appears when AmB concentration increases [4]. Both monomeric and aggregated forms of AmB interact with ergosterol in fungal membranes, forming transmembrane pores through which a leakage of ions and metabolites occurs. However, only aggregated forms produce such pores in mammalian cell membranes that are rich in cholesterol [5]. Currently available formulations of AmB for clinical applications include Fungizone® and lipid formulations consisting of AmBisome®, Amphotec™ and Abelcet®. Fungizone® is essentially a colloidal dispersion in which AmB is solubilized with sodium deoxycholate; however, AmB is released rapidly from Fungizone® in the aggregated form upon dilution in plasma, leading to severe side effects, which limit its widespread clinical applications [6,7]. Although lipid formulations of AmB are less toxic than Fungizone®, the side effects and pharmacokinetic profiles of each formulation are highly variable and pose difficulties in dose titration [8,9]. In general, the high cost and dose requirements are major limitations of currently available lipid-based systems [10]. Thus, there is an imperative unmet need to develop innovative and cost-effective formulations of AmB with reduced toxicity.

Polymeric micelles are promising drug carriers for the delivery of hydrophobic therapeutics. Due to the unique core/shell structure, polymeric micelles not only enhance water solubility but also reduce non-specific toxicities of loaded drugs [11]. In addition, various covalent/non-covalent interactions can be introduced into polymeric micelles systems to improve drug-micelle interaction and drug-loading capacity, enhance systemic stability and achieve controlled drug release [11]. Some reports have shown that loading AmB into micelles could reduce the aggregation forms of AmB, thus significantly lowering the toxicities [10,12–15]. For instance, Adams and his coworker encapsulated AmB into micelles using poly(ethylene oxide)-*block*-poly(N-hexyl-L-aspartamide) having acyl side chains, and demonstrated a reduced degree of aggregation and hemolysis compared with free AmB in solution due to the interaction between AmB and the acyl chains [16].

In recent years, polycarbonate polymers have been widely explored in drug delivery due to their biodegradability, low toxicity *in vivo*, and easy functionalization [17]. In this study, polymeric micelles were developed using phenylboronic acid-functionalized polycarbonate/PEG diblock copolymers for the delivery of AmB to reduce non-specific toxicity without appreciable loss in antifungal activity. In an attempt to inhibit self-aggregation of AmB and achieve controlled drug release, boronic acid groups included may potentially interact with AmB *via* hydrogen-bonding and ionic interactions. Boronate ester bond formation via phenylboronic acid interaction with diols may also contribute to this effect [18]. As a comparison, urea-functionalized polycarbonate/PEG diblock copolymer (PEG-PUC) was employed to prepare AmB-loaded and mixed micelles with PEG-PBC. The AmB-loaded micelles were prepared using a sonication-dialysis method and characterized *via* particle size, size distribution, TEM and *in vitro* stability. Additionally, the *in vitro* drug release and aggregation status of AmB in the different micelle formulations were assessed. Lastly, antifungal effects and hemolytic activity were evaluated and compared with free AmB as well as Fungizone® *in vitro*.

2. Materials and methods

2.1. Materials

Amphotericin B, dimethylsulfoxide (DMSO, synthesis grade, 99.9%), Tween 80, Triton X-100 and Mueller Hinton agar were acquired from Sigma-Aldrich (St Louis, MO, USA). Fungizone® was purchased from Invitrogen Gibco containing 250 μg of amphotericin B and 205 μg of sodium deoxycholate per mL of distilled water. YM broth (Acumedia No. 7363A) was purchased from Neogen Corporation (Michigan, USA). Phosphate-buffered saline (PBS) solution at 10 × concentration was purchased from Vivantis Technologies (Malaysia) and diluted appropriately before use. Methyl-PEG (mPEG) (Mn 10000 g/mol, polydispersity index-PDI: 1.10) was obtained from Polymer Source Inc. (Canada), lyophilized and transferred to a glove-box one day prior to use. 1,8-Diazabicyclo[5,4,0]undec-7-ene (DBU) was dried over CaH_2 overnight, and dried DBU was obtained after vacuum distillation before being transferred to a glove-box prior to use. 6 mm antibiotic assay discs (2017-006) were purchased from GE Healthcare Life Sciences (Singapore). Rat red blood cells (rRBCs) were obtained from the Animal Handling Units of the Biomedical Research Centers (AHU, BRC, Singapore).

2.2. Synthesis and characterization of monomers and diblock copolymers

The synthesis and characterization of PEG-PUC were performed using a previously published protocol [19]. The details for synthesizing phenylboronic acid-functionalized monomer (MTC-PBA) and PEG-PBC were provided below (Scheme 1). All polymerization reactions were carried out in a glove-box under nitrogen atmosphere.

2.2.1. MTC-PBA

In a dry two-neck 500 mL round bottom flask equipped with a stir bar, MTC-OH (3.08 g, 19.3 mmol) was dissolved in dry tetrahydrofuran (THF) (50 mL) with 5–8 drops of dimethylformamide (DMF). Subsequently, oxalyl chloride (3.3 mL) was added in one shot (pure form), followed by additional of THF (20 mL). The solution was stirred for 90 min, after which volatiles were dried under a strong flow of nitrogen to yield a pale yellow solid intermediate (5-chlorocarboxy-5-methyl-1,3-dioxan-2-one, MTC-Cl). The solid was then subjected to heat at 60 °C for 2–3 min for removal of the residual solvent, and re-dissolved in dry dichloromethane (CH_2Cl_2, 50 mL). The flask was immersed in an ice bath at 0 °C. A mixture of 4-(hydroxymethyl) phenylboronic acid pinacol ester (4.19 g, 17.88 mmol) and triethylamine (1.77 mL, 19.3 mmol) were dissolved in dry CH_2Cl_2 (50 mL), which was added dropwise to the flask over a duration of 30 min. The flask was removed out of the ice batch, allowing the reaction to proceed at room temperature (~22 °C) for 2.5 h under stirring. The reaction was then quenched by addition of 50 mL of brine, and the organic phase was collected after separation. After removal of the solvent, the crude product was purified by silica-gel flash column chromatography *via* a hexane-ethyl acetate solvent system (gradient elution up to 20% vol. ethyl acetate) followed by a solvent switch to dichloromethane-ethyl acetate (gradient elution up to 20% vol. ethyl acetate) to yield MTC-PBA as a white solid. The product was further purified by recrystallization. The solid was dissolved in 50 mL of diethyl ether and the residues were filtered. The filtrate was dried and subsequently dissolved in 2 mL of diethyl ether and ethyl acetate (1 mL each), followed by addition of 50 mL of hexane. The crystals were allowed to form at room temperature for 1 day, and subsequently obtained by washing the crystals with cold hexane. ^{1}H NMR (400 MHz, $CDCl_3$, 22 °C): δ 7.83–7.32 (m, 4H, —C_6H_4B═), 5.22 (s, 2H, —$CH_2C_6H_4$—), 4.72–4.18 (m, 4H, —$COOCH_2$—), 1.34 (s, 12H, —$OC(CH_3)_4CO$—), 1.32 (m, 3H, —CH_3).

2.2.2. PEG-PBC

In a glove-box, 0.222 g (0.022 mmol) of 10 kDa mPEG-OH initiator and 0.376 g (1 mmol) of MTC-PBA were charged in a 20 mL

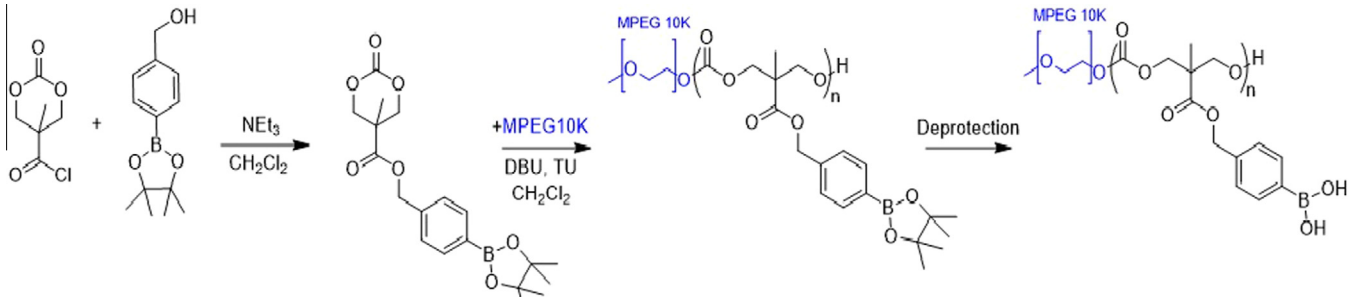

Scheme 1. Synthesis of diblock copolymer of PEG-PBC.

glass vial equipped with a stir bar. Dichloromethane was added and the monomer concentration was adjusted to 2 M. Once the initiator and monomer were completely dissolved, 8.3 μL (0.06 mmol) of DBU was added to initiate the polymerization. After 3.5 h of stirring at room temperature, the reaction was quenched with 30 mg of benzoic acid under stirring for 5 min. Subsequently, the polymer intermediate was purified *via* precipitation twice in cold diethyl ether, and dried on a vacuum line until a constant weight was achieved. ^{1}H NMR (400 MHz, $CDCl_3$, 22 °C): δ 7.83–7.27 (m, 48H, —C_6H_4B═), 5.23–5.02 (m, 24H, —$CH_2C_6H_4$—), 4.49–4.13 (m, 48H, —$COOCH_2$—), 3.84–3.43 (m, 908H, —OCH_2CH_2— from 10 kDa PEG), 3.38 (s, 3H, CH_3-PEG-), 1.39–1.27 (m, 144H, —$OC(CH_3)_4CO$—), 1.26–1.16 (m, 36H, —CH_3).

The protected polymer was then deprotected by dissolving in 14 mL of methanol and THF (1:1). Ten equivalents (with respect to mols of protected phenylboronic pinacol pendant groups) of benzene-1,4-diboronic acid and Amberlyst® 15 acidic resins were added to a 50 mL round bottom flask containing the protected polymer. The flask was subsequently heated to 50 °C with overnight stirring. After that, the solvents were removed under vacuum. The deprotected polymer was dissolved in 10 mL of isopropanol and acetonitrile (1:1) and placed in a dialysis bag of 1000 MW cut-off. Dialysis was carried out for 2 days at room temperature using 1:1 isopropanol and acetonitrile. Finally, the solvents were removed, and the polymer was lyophilized to obtain an off-white polymer. ^{1}H NMR (400 MHz, DMSO-d_6, 22 °C): δ 8.22–7.88 (m, 24H, —$B(OH)_2$), 7.84–7.15 (m, 48H, —C_6H_4B═), 5.23–4.96 (m, 24H, —$CH_2C_6H_4$—), 4.46–4.02 (m, 48H, —$COOCH_2$—), 3.71.-3.14 (m, 909H, —OCH_2CH_2— from 10 kDa PEG), 3.23 (s, 3H, CH_3-PEG-), 1.25–1.05 (m, 36H, —CH_3).

2.2.3. Characterization of PEG-PBC

^{1}H NMR spectrum was obtained on a Bruker Avance 400 instrument at 400 MHz. Gel permeation chromatography (GPC) was performed in THF using a Waters system equipped with four increasing pore size (100, 1000, 105, and 106 Å), a Waters 410 differential refractometer, and a 996 photodiode array detector. The system was calibrated with polystyrene standards.

2.3. Determination of critical micelle concentration (CMC)

The CMC values of PEG-PBC, PEG-PUC and the mixture of PEG-PBC and PEG-PUC were measured using previously reported method [20]. Briefly, 10 μL of pyrene acetone solution at concentration of 6.16×10^{-5} M was added into glass vials and allowed the acetone to evaporate under room temperature. Subsequently, 1 mL of polymer solution at concentrations ranging from 0.01 to 1000 mg/L was added into each vial. After mixing, the mixture solutions were incubated overnight and then scanned from 300 to 360 nm with an emission wavelength of 395 nm to acquire excitation spectra using a LS50B luminescence spectrometer (Perkin Elmer, U.S.A). The excitation and emission bandwidths were both set at 2.5 nm. The CMC value was calculated based on the curve plotted using the intensity ratios of I337/I334 for different polymer concentrations as a function of polymer concentration.

2.4. Micelles preparation and characterizations

AmB-loaded micelles were formed using the sonication-dialysis method (Scheme 2). Briefly, 5 mg of AmB was dissolved in 1 mL of DMSO. Subsequently this solution was added to 1 mL of DMSO containing 10 mg of polymers (PEG-PBC, PEG-PUC or mixture of PEG-PBC and PEG-PUC at 1:1 molar ratio) and incubated at room temperature for 30 min. The mixture solution was added dropwise into 10 mL DI water within 2 min while being sonicated (130 W, Vibra Cell VCX 130) in an ice bath. The sample was then subjected to dialysis against DI water for 48 h to remove free AmB and organic solvent. The water was changed at 6, 24 and 30 h. The micelles were collected for further analysis. The concentration of copolymers was approximately 0.7 mg/mL in the micellar formulations.

The particle size, size distribution and zeta potential of the micelles were characterized by DTS zetasizer Nano (Malvern Instruments, UK). The morphology of the micelles was visualized by transmission electron microscopy (TEM, FEI Tecnai G2 F20 electron microscopy) using an acceleration voltage of 200 keV. Briefly, one drop of micelle solution (4 μL) was added onto a Formvar coated 200 mesh copper grid (Ted Pella Inc., U.S.A.). After 1 min, the excess solution was removed by filter paper. Same volume of phosphotungstic acid (1%) was added onto the grid, and the excess solution removed after 1 min. The grid was left to dry under room temperature.

The stability of the micelles was evaluated by monitoring the changes of particle size as a function of time at 200 mg/L in PBS (pH 7.4) at 4 °C and in PBS (pH 7.4) containing 10% FBS at 37 °C, respectively. The change of scattered light intensity, in the presence of sodium dodecyl sulfate (SDS, 2.23 mg/mL) at room temperature, was recorded using DTS zetasizer Nano at predetermined time points to evaluate the kinetic stability of the micelles.

2.5. Determination of encapsulation efficiency and study of aggregation state of AmB in the micelles

The drug encapsulation efficiency (EE%) of the micelles was determined using High-performance liquid chromatography (HPLC) (Shimadzu, Kyoto) according to a published protocol [21] and calculated using the following formula: EE% = (mass of drug loaded in micelles/mass of initial loaded drug) × 100%.

The aggregation state of AmB in micelles was analyzed by using UV–Vis spectroscopy (Ultrospec 2100 Pro, Amersham). The AmB concentration was adjusted to 25 mg/L. As comparison, solution of Fungizone® diluted in PBS and AmB dissolved in DMSO were

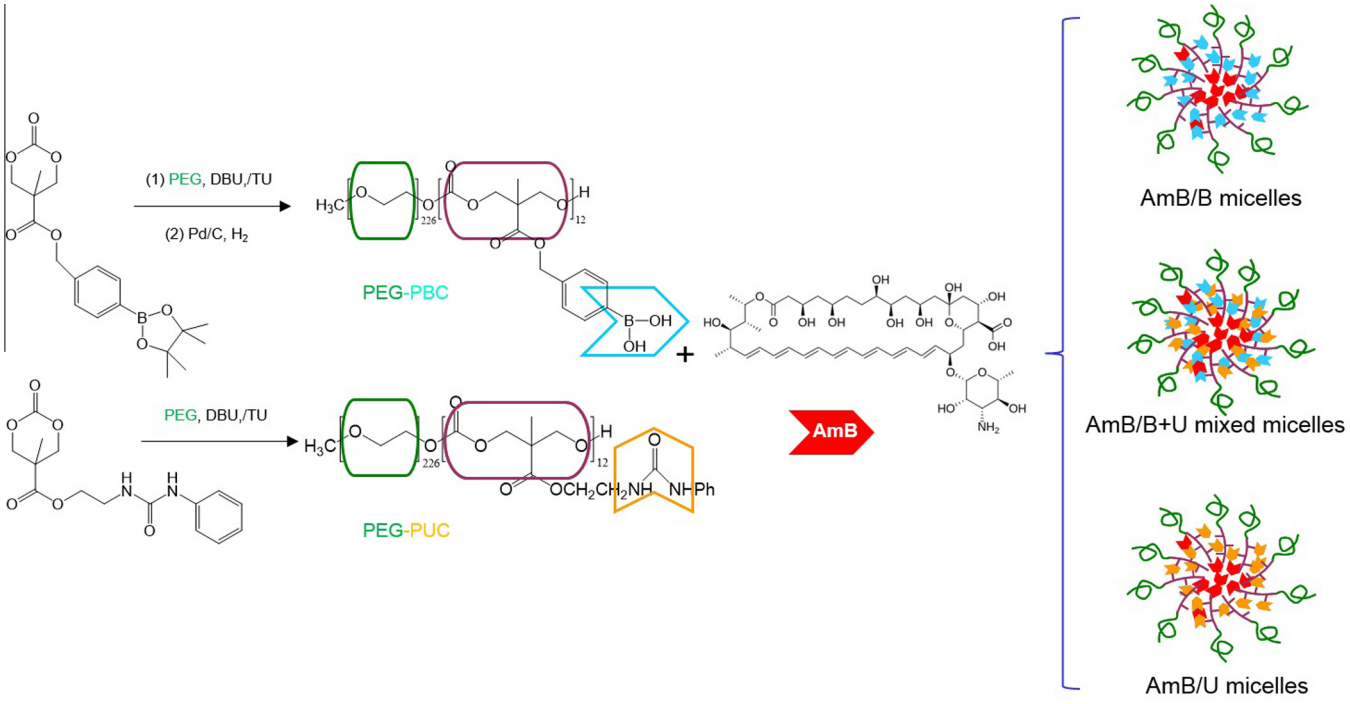

Scheme 2. Schematic showing of AmB-loaded micelles preparation using PEG-PBC and PEG-PUC.

also prepared. The spectra of different samples were acquired from 300 to 450 nm.

2.6. In vitro drug release

The *in vitro* release of AmB from micelles was investigated by dialysis against PBS at pH 7.4 at 37 °C. Briefly, AmB-loaded micelle, Fungizone® or free AmB solution (1 mg/L, 2 mL) was introduced into a dialysis bag (Molecular weight cut-off, 11 kDa) and then immersed into 20 mL of PBS (pH 7.4) containing 1% tween 80 while being shaken at 100 rpm. At the predetermined time points, the release medium was collected and replaced with the same volume of PBS. The content of AmB release was measured using HPLC.

2.7. In vitro antifungal activity

To evaluate the *in vitro* antifungal activity of various formulations, firstly the minimal inhibitory concentration (MIC) against *C. albicans* (ATCC No. 10231) was determined using an established protocol [22]. Briefly, 100 μL of diluted AmB-containing formulations including micelles, free AmB, Fungizone® (AmB concentrations ranged from 0.06–7.8 mg/L) and blank micelle (polymer concentrations ranged from 3.9–1000 mg/L) solutions, were added to an equal volume of fungal solution containing approximately 10^5 CFU/mL in a 96-well plate. The plate was incubated at 37 °C under shaking at a speed of 200 rpm. After 42 h, the optical density (OD) at 600 nm was read using a microplate reader (TECAN, Switzerland).

The disk diffusion test was also performed to assess the *in vitro* antifungal effects of various formulations [23]. Briefly, the turbidity of *C. albicans* culture was adjusted to an OD reading of 0.07. The yeast solution (300 μL) was spread onto MH agar plate, and allowed to be absorbed for 10 min. The paper discs (6 mm) presoaked in different samples at a concentration of 31.25 mg/L were placed gently onto the agar plate. The plate was inverted and incubated at 37 °C. The zone diameter of inhibition was measured after 24 h of incubation. The disk impregnated with growth media was used as control.

2.8. Hemolysis assay

To evaluate the toxicity of the AmB-loaded micelles as compared to free AmB and Fungizone®, their hemolytic activity was tested against rat red blood cells (rRBCs) using a previously reported method with slight modification [24]. The rRBCs were diluted 25 times with PBS (pH 7.4). Serial two-fold dilution of the micelles, free AmB and Fungizone® was prepared using PBS (0.39–25 mg/L). The drug solution (250 μL) at different concentrations was gently mixed with an equal volume of the blood suspension. The mixtures were centrifuged at 4000 *g* for 5 min after 1 h incubation at 37 °C. After centrifugation, 100 μL of the supernatant was transferred into a 96-well plate. The rRBCs treated with PBS served as a negative control while the rRBCs treated with 1% Triton-X were used as a positive control. The absorbance of hemoglobin released was read at 576 nm using the microplate reader (TECAN, Switzerland). The hemolysis was calculated based on following formula: Hemolysis (%) = [(O.D.$_{576nm}$ of treated sample − O.D.$_{576nm}$ of negative control)/(O.D.$_{576nm}$ of positive sample − O.D.$_{576nm}$ of negative control)] × 100%.

In addition, the hemolysis induced by AmB-loaded micelles at a fixed concentration of 12.5 mg/L and blank micelles was also monitored as a function of time. The samples were incubated at 37 °C and the hemolysis was determined at predetermined time points (1, 2, 4, and 6 h). Each test was carried out in 4 replicates and reproduced twice.

2.9. Study of in vivo nephrotoxicity

The *in vivo* nephrotoxicity of Fungizone® and AmB-loaded micelles was evaluated in a mouse model. Briefly, healthy BALB/c mice (female, body weight 19–25 g) were randomly divided into 4 groups of 3 mice each. AmB/B micelles, AmB/B+U mixed micelles and Fungizone® were injected through tail vein at a dose of

1 mg/kg for 3 consecutive days [25]. Two days after the last injection, the mice were sacrificed and the kidneys excised. The samples were fixed using 10% formalin followed by paraffin embedding and terminal deoxynucleotidyl transferase-mediated dUTP nick-end labeling (TUNEL) staining. The nuclei were visualized by counterstaining the slides with hematoxylin. The number of TUNEL-positive nuclei in 9 representative fields (3 fields from each mouse) was counted to determine the apoptotic cells in the kidney sections. The images were acquired using a light microscope (Olympus, Japan). Animal studies were carried out according to the protocols approved by the Singapore Biological Research Center (BRC)'s Institutional Animal Care and Use Committee.

2.10. Statistical analysis

Data were presented as means ± standard deviation (SD). Data were analyzed using one-way ANOVA followed by Tukey's post hoc analysis (Graphpad, Prism, USA). The difference between values for the treatments was considered to be statistically significant at $p < 0.05$.

3. Results and discussion

3.1. Synthesis of phenylboronic acid-functionalized monomer and diblock copolymer

MTC-urea monomer and diblock copolymer PEG-PUC were prepared following previously established protocols [19]. The phenylboronic acid-functionalized monomer (MTC-PBA) was synthesized by direct coupling of MTC-Cl and 4-hydroxymethyl phenylboronic pinacol in the presence of trimethylamine with a yield of 52% after column and recrystallization. The diblock copolymer, PEG-PBC, was synthesized *via* metal-free organocatalytic ROP of MTC-PBA using mPEG of 10 kDa as a macroinitiator in the presence of the catalyst DBU (Fig. 1a) for 3.5 h. ^{1}H NMR integration values of monomers relative to the PEG initiator correlated well, confirming

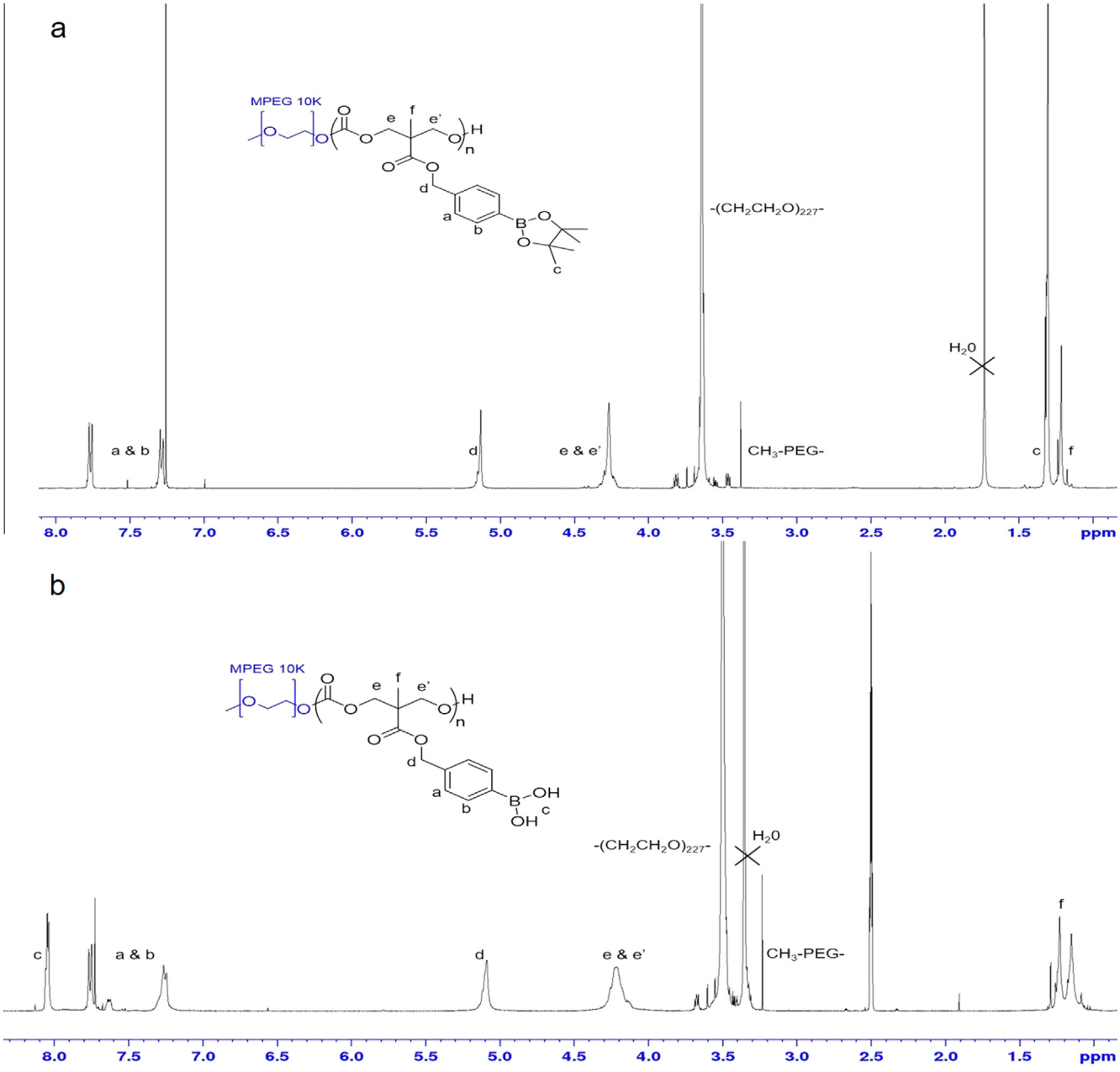

Fig. 1. ^{1}H NMR of (a) pinocal protected PEG-PBC and (b) PEG-PBC.

controlled polymerization and predictable molecular weights *via* initial monomer to initiator feed ratio. In addition, the proton NMR analysis displayed all the peaks associated with both initiator and monomers (Fig. 1a). From the GPC results, the polymer had narrow molecular weight distribution (PDI 1.16). The pinacol protected phenylboronic acid groups in the polymers were deprotected at 50 °C using benzene-1,4-diboronic acid and acidic resins. The proton NMR analysis of the deprotected polymer showed 97% deprotection of the pinacol protecting groups, demonstrating efficient deprotection. In addition, the presence of a new distinct peak at δ 8.05 ppm confirmed the presence of hydroxyl groups, which correlated to the deprotected phenylboronic acid pendant groups (Fig. 1b).

3.2. Characterization of AmB-loaded micelles

CMC refers to the lowest concentration for copolymer to self-assemble into micelles, a parameter reflecting thermodynamic stability [20]. The PEG-PBC polymer, the mixture of PEG-PUC/PEG-PBC (1:1 molar ratio) and PEG-PUC polymer presented low CMC values (8.0, 4.3 and 3.8 mg/L), indicating the micelles formed by these polymers potentially have high thermodynamic stability. Blank micelles were formed by self-assembly in water with small particle size and low PDI based on the dynamic light scattering (DLS) analysis (Fig. 2a). The AmB-loaded micelles, *i.e.*, AmB/B micelles, AmB/B +U mixed micelles, and AmB/U micelles, showed slightly larger particle sizes than the corresponding blank micelles, which were all well below 100 nm, ideal for *in vivo* application (Fig. 2a). All the AmB-loaded micelles demonstrated narrow size distribution, as suggested by the PDI values: 0.17 ± 0.01, 0.18 ± 0.01 and 0.16 ± 0.04 for AmB/B, AmB/B+Uand AmB/U micelles, respectively (Fig. 2a). The morphologies of the micelles were visually observed under TEM. The dimensions of the micelles from the TEM analysis were generally in agreement with the DLS analysis (Fig. 2b–d). All the micelles had zeta potential values close to neutral (−1.6 ± 2.0 mV, −2.4 ± 1.5 mV and −2.0 ± 0.5 mV for AmB/B, AmB/B+U and AmB/U micelles, respectively) (Fig. 2a). The electrically neutral surface of nanoparticles is ideal for *in vivo* systemic application to avoid aggregate formation with serum proteins typically observed with highly cationic nanoparticles, as well as rapid uptake by phagocytic cells resulting in fast clearance from the blood observed with highly anionic counterparts [26,27]. In addition, as shown in Fig. 3a and b, AmB/B micelles and AmB/B+U mixed micelles exhibited higher stability in both PBS (pH 7.4, 4 °C) and serum-containing PBS (pH 7.4, 37 °C) over 14 days and 5 days, respectively, as compared to AmB/U micelles. In the presence of SDS which acted as a destabilizing agent, AmB/B micelles displayed significantly greater kinetic stability than AmB/B+U mixed micelles and AmB/U micelles (relative intensity at 48 h: 74.1 ± 0.4% *vs* 45.8 ± 1.2% and 6.6 ± 0.1%) (Fig. 3c). The phenylboronic acid groups in PEG-PBC could form hydrogen-bonding, boronate ester bond and ionic interactions with amine group in AmB, thus enhancing stability of AmB-loaded micelles. However, the urea functional groups in the PEG-PUC had strong tendency to undergo self-association *via* hydrogen-bonding [28,29]; consequently resulting in reduced interactions between the PEG-PUC polymer and AmB. In addition, urea group might compete with amine group in AmB for interacting with boronic acid *via* hydrogen-bonding interaction, which might be the reason for the compromised stability of AmB/B+U micelles as compared to AmB/B micelles.

a

Micelles	Size (nm)	PDI	Zeta Potential (mV)	Encapsulation Efficiency (%)	CMC (mg/L)
B blank micelles	38.1 ± 1.6	0.06 ± 0.01	-1.4 ± 1.1	NA	8.0
B+U blank micells	39.3 ± 0.7	0.10 ± 0.01	-1.2 ± 0.3	NA	4.3
U blank micelles	53.6 ± 1.8	0.13 ± 0.01	-0.6 ± 0.3	NA	3.8
AmB/B micelles	54.5 ± 0.3	0.17 ± 0.01	-1.6 ± 2.0	66.4 ± 3.6	NA
AmB/B+U mixed micelles	56.9 ± 0.5	0.18 ± 0.01	-2.4 ± 1.5	72.2 ± 4.4	NA
AmB/U micelles	84.8 ± 0.7	0.16 ± 0.04	-2.0 ± 0.5	76.4 ± 1.4	NA

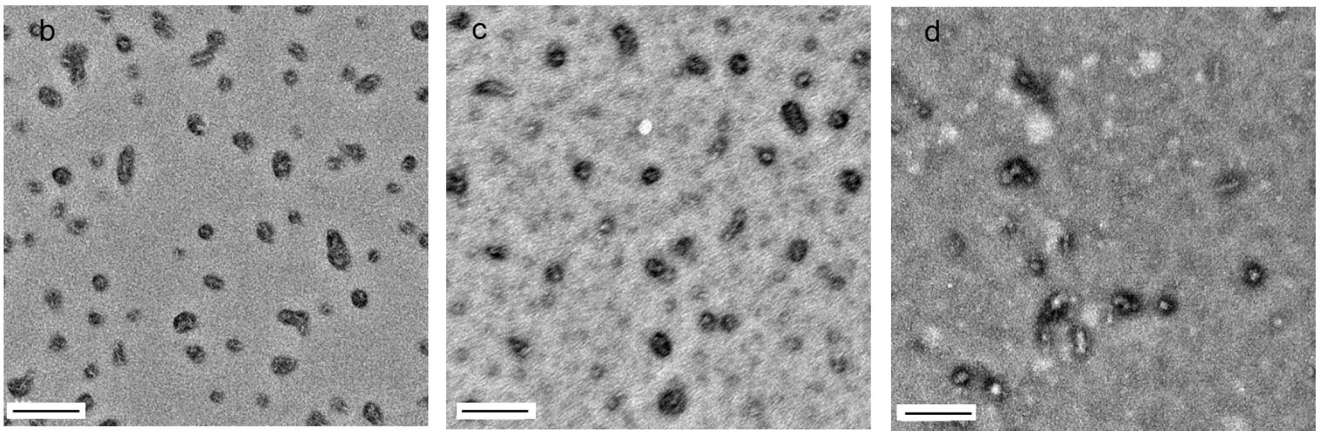

Fig. 2. Characterization of micelles: (a) Size, PDI, zeta potential, encapsulation efficiency and CMC for AmB-loaded micelles and blank micelles; Morphology observed under TEM images: (b) AmB/B micelles, (c) AmB/B+U mixed micelles, and (d). AmB/U micelles, scale bar: 100 nm.

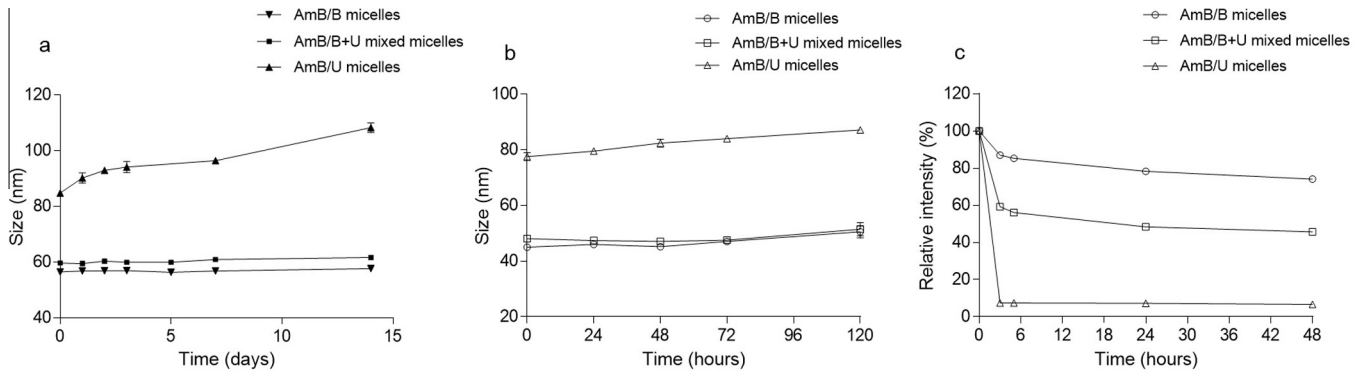

Fig. 3. Stability of various AmB-loaded micelles in PBS (pH 7.4) at 4 °C (a), in 10% FBS containing PBS (pH 7.4) at 37 °C (b), and in the presence of SDS (c). Error bars obtained are smaller than the marker.

3.3. Encapsulation efficiency and aggregation state of AmB in the micelles

All the micelles displayed satisfactory drug encapsulation efficiencies: 66.4 ± 3.6%, 72.2 ± 4.4% and 76.4 ± 1.4% for AmB/B micelles, AmB/B+U mixed micelles and AmB/U micelles, respectively (Fig. 2a). As the absorption spectrum of AmB is highly sensitive to its local environment [30], the aggregation state of AmB was determined by absorption spectroscopy. Fig. 4 shows the UV spectra of AmB in Fungizone®, in DMSO and in various micelles. Band IV located at 407–419 nm is the characteristic peak for monomeric form of AmB, while Band I at approximately 330–340 nm represents the aggregated form [8]. As can be seen from Fig. 3, the spectra of AmB DMSO solution demonstrated the non-aggregated state of AmB with prominent bands II, III and IV at 371, 391, and 414 nm, respectively. In contrast, AmB was highly aggregated in Fungizone®, resulting in a loss of monomer absorbance at 414 nm (Band IV) and an increased absorbance at 329 nm (Band I). A similar spectra pattern was observed for AmB/U micelles, demonstrating that due to the poor interaction between urea functional groups and AmB, encapsulation of AmB using PEG-PUC polymer alone failed to reduce the aggregation extent of the drug. Whereas for AmB/B micelles and AmB/B+U mixed micelles, Band I (329 nm) was found to have red-shifted towards 345–355 nm region and merged partially with Band II, indicating a reduction in AmB self-aggregation [31]. These results were supported by enhanced monomer absorption as shown by the increased intensity of band IV for AmB/B micelles and AmB/B+U mixed micelles. The ratio of intensity of band I to band IV (*i.e.*, I/IV ratio) was used to evaluate the degree of AmB aggregation [32]. The I/IV ratios for Fungizone® and AmB/U micelles were as high as 6.4 and 6.3, respectively, while for AmB/B micelles, the ratio dropped drastically to 1.1. This indicates that compared to Fungizone®, AmB/B micelles significantly reduced the aggregation status of AmB, while AmB/U micelles had no effect. AmB/B+U mixed micelles, however, exerted an intermediate effect with a ratio of 2.4. These findings suggest that the aggregation state of AMB is dependent on the presence of phenylboronic acid functional groups which serve to bind AmB in its monomeric state *via* hydrogen-bonding, boronate ester bonding, and ionic interaction in the micellar formulations. The reduction in aggregation state of AmB in the micelles is potentially beneficial for systemic application due to lowered cytotoxicities.

3.4. In vitro drug release

In vitro AmB release from various micellar formulations were determined and compared with free AmB solution and Fungizone®. As shown in Fig. 5, AmB/U micelles displayed a burst drug release profile similar to that of free AmB and Fungizone® over 24 h. The percentages of AmB released from Fungizone®, free AmB and AmB/U micelle formulations were 98.7 ± 3.4%, 96.2 ± 2.5% and 86.6 ± 1.9%, respectively. In contrast, a sustained drug release profile was observed for both AmB/B micelles and AmB/B+U mixed micelles, with 48.6 ± 2.1% and 59.2 ± 1.8% of the loaded AmB

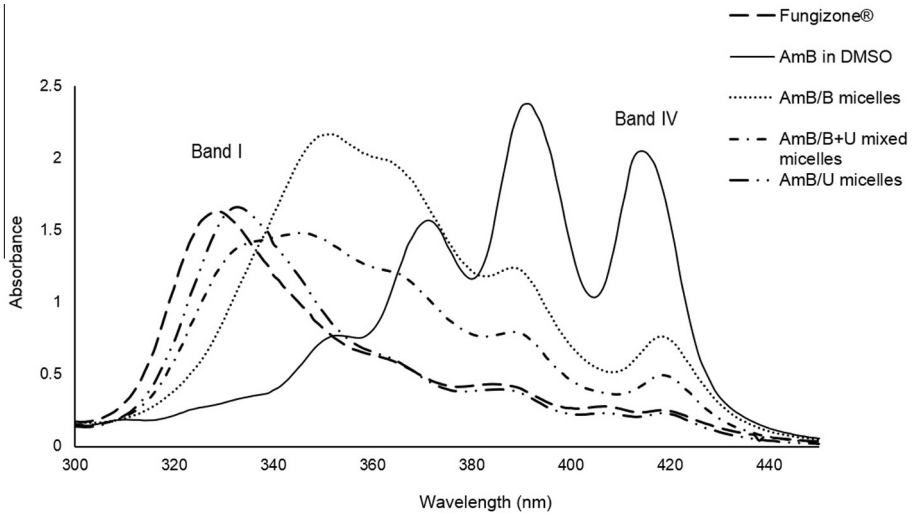

Fig. 4. Absorbance spectra of AmB-loaded micelles, Fungizone® and free AmB in DMSO.

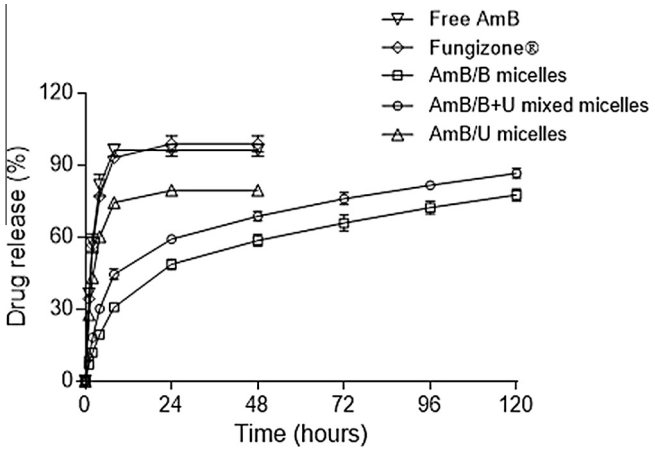

Fig. 5. *In vitro* release of AmB from AmB/B micelles, AmB/B+U mixed micelles, AmB/U micelles, free AmB solution and Fungizone® in PBS (pH 7.4) at 37 °C. Error bars obtained are smaller than the marker.

Table 1
MICs of free AmB, Fungizone®, drug-loaded micelles and blank micelles against *C.albicans.*

Formulation	MIC (mg/L)
Free AmB	0.24
Fungizone®	0.24
AmB/B micelles	0.96
AmB/B+U micelles	0.48
AmB/U micelles	0.24
B blank micelles	>1000
B+U blank micelles	>1000
U blank micelles	>1000

released by 24 h, respectively. These results indicate that physical entrapment of AmB using the PEG-PUC polymer exerted no control over drug release. However, due to the interactions between phenylboronic acid groups and AmB, the release of AmB could be better controlled, avoiding high drug concentration caused by rapid release, which is ideal for minimizing the toxicity induced by exposure of aggregated AmB to mammalian cells.

3.5. In vitro antifungal activity

To evaluate the *in vitro* antifungal activity of various formulations, MIC was determined against *C. albicans*, which is commonly susceptible to AmB. As Table 1 shows, AmB/U micelles and AmB/B+U mixed micelles exhibited comparable MIC values (0.24 mg/L and 0.48 mg/L) to free AmB and Fungizone® (0.24 mg/L for both), while AmB/B micelles were slightly less effective than the aforementioned formulations (MIC: 0.96 mg/L). The disk diffusion assay showed similar results (Fig. 6): AmB/U micelles and AmB/B+U mixed micelles promoted microbial growth inhibition haloes (diameter: 1.33 ± 0.10 and 1.28 ± 0.05 cm, respectively) that were comparable to those formed by Fungizone® and free AmB (diameter of 1.38 ± 0.05 and 1.43 ± 0.10 cm, respectively) ($p > 0.05$). AmB/B micelle induced a halo with diameter of 1.05 ± 0.06 cm, which was significantly smaller than Fungizone® ($p < 0.05$). A plausible explanation for the different *in vitro* antifungal activity of the AmB-loaded micelles could be associated with the *in vitro* drug release profiles. As discussed previously, we attribute the relative weaker *in vitro* antifungal effect of AmB/B micelles to slower drug release resulting from strong interactions between phenylboronic acid groups and AmB. By adding PEG-PUC polymer to reduce such interactions, the mixed micelles are expected to display improved efficacy due to greater drug availability from more rapid drug release.

3.6. In vitro and in vivo toxicity

Hemolysis is a common parameter for evaluating the *in vitro* toxicity of AmB [33]. After incubation for 1 h, as shown in Fig. 7a free AmB, Fungizone® and AmB/U micelles (25 mg/L) resulted in 89.7 ± 1.3%, 78.7 ± 1.8% and 52.0 ± 1.0% of hemolysis, respectively, which can be attributed to both the rapid drug release and high aggregated AmB content of these formulations. In sharp contrast, the AmB/B micelles and AmB/B+U mixed micelles caused little or no hemolysis during the same period. From Fig. 7b, it can be seen that AmB/B micelles delayed the onset of hemolysis to 4 h at a low hemolysis degree (10.0 ± 0.3%). Similarly, a delayed onset (2 h) and reduced degree of hemolysis was also observed for AmB/B+U mixed micelles as compared to free AmB and Fungizone®. In contrast, AmB/U micelles failed to delay the onset of hemolysis even though it caused slightly lower extent of hemolysis

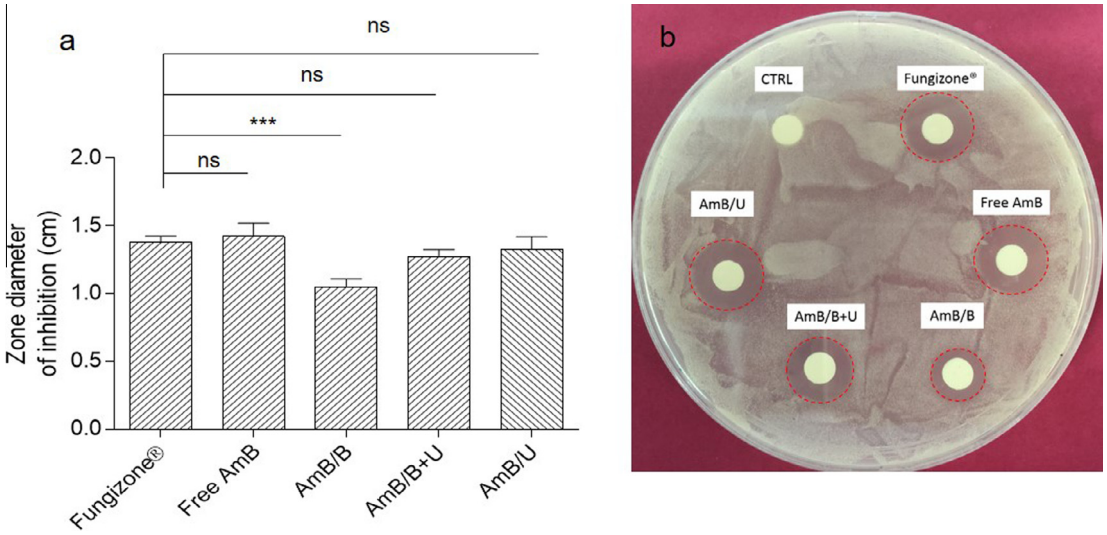

Fig. 6. The zone of inhibition diameters of free AmB, Fungizone® and AmB-loaded micelles (a) and an illustrative image (b). "***" denotes $p < 0.001$ and "ns" denotes no significant difference.

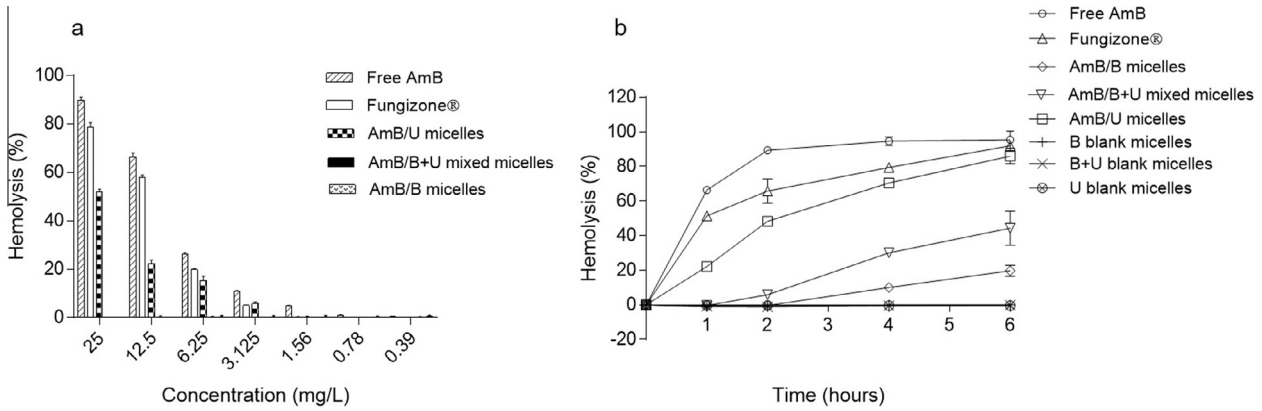

Fig. 7. Effect of hemolysis of free AmB, Fungizone® and AmB-loaded micelles: (a) after 1 h incubation at various concentrations and (b) as function of time at concentration of 12.5 mg/L. Error bars obtained are smaller than the marker.

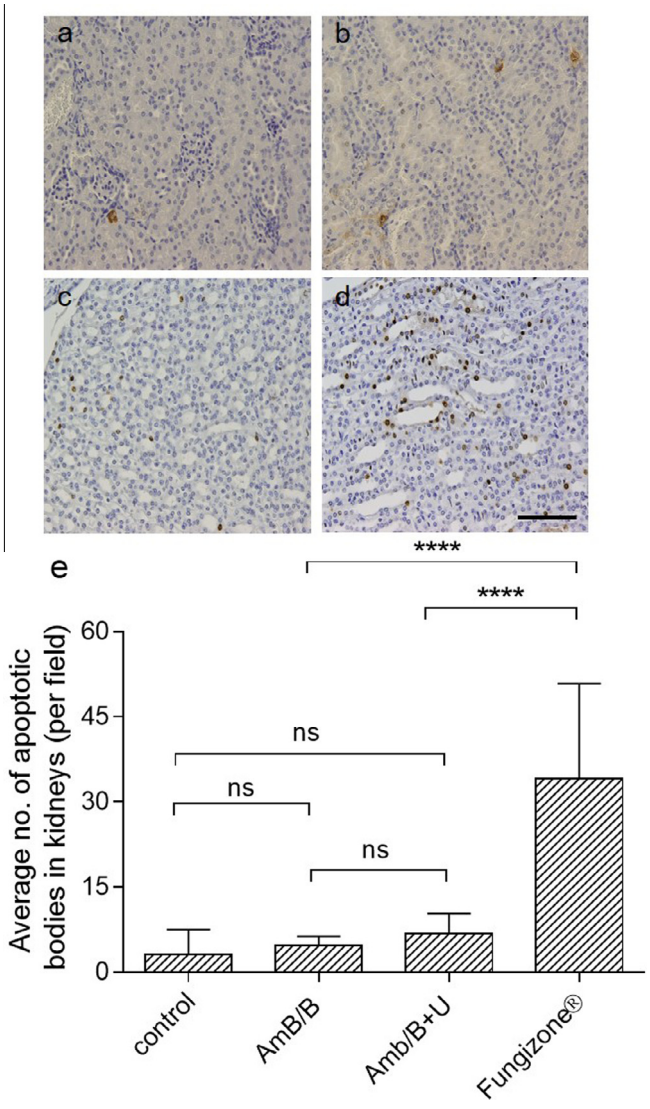

Fig. 8. TUNEL staining of kidney tissues at 2 days post-injection of AmB-loaded micelles and Fungizone®. Kidney sections obtained from mice treated with (a) control (PBS); (b) AmB/B micelles; (c) AmB/B+U mixed micelles, and (d) Fungizone®; quantification of mean apoptotic bodies per field (objective × 20) in kidney tissues ("****" denotes $p < 0.0001$, "ns" denotes no significant difference). Scale bar: 100 μm.

compared with free AmB and Fungizone®. Similar to antifungal activity, the varied hemolytic profiles for the various AmB-loaded micelles is likely due to the differences in AmB aggregation degree and drug release pattern. Despite its relatively weaker antifungal efficacy, AmB/B micelles presented a favorable toxicity profile in this study due to the significantly slower drug release and higher AmB monomer content compared to other formulations. Similar to the findings of *in vitro* antifugal study, the AmB/B+U mixed micelles also demonstrated an intermediate hemolysis profile due to the reduced interaction between PEG-PBC and AmB caused by the addition of PEG-PUC.

The nephrotoxicity of Fungizone® and AmB-loaded micelles in mice was investigated using histological examination of kidney excised from the mice. Using the TUNEL assay, the apoptotic cells were quantified by counting the brown regions that formed due to the apoptosis [34]. Fig. 8a–d shows that the treatment of Fungizone® led to significantly higher number of apoptotic cells in the kidneys as compared to AmB/B micelles and AmB/B+U micelles ($p < 0.0001$); there was no significant difference among the numbers of apoptotic cells caused by AmB/B micelles, AmB/B+U mixed micelles and control ($p > 0.05$). These results further proved that unlike Fungizone®, AmB/B micelles and AmB/B+U mixed micelles did not induce significant nephrotoxicity.

4. Conclusion

In this study, we have employed the application of phenylboronic acid-functionalized polycarbonate/PEG diblock copolymers for the encapsulation of poorly soluble and toxic antifungal drug AmB *via* hydrogen-bonding, boronate ester formation, ionic and hydrophobic interactions. Three types of micelles, AmB/B micelles, AmB/B+U mixed micelles and AmB/U micelles, were prepared, characterized, and evaluated for their toxicity and antifungal activity. The non-covalent interactions between phenylboronic acid functional groups and AmB conferred AmB/B micelles an excellent stability under various conditions, a reduction in AmB aggregation and a controlled drug released profile, which effectively translated into a delayed and reduced degree of hemolysis and mitigation of nephrotoxicity. This occurred however at a slight expense of antifungal activity when compared to free AmB and Fungizone®. On the other hand, urea-functionalized diblock copolymer, PEG-PUC, displayed a tendency to undergo self-association due to strong hydrogen-bonding interactions between urea groups, and resulted in poor interactions with AmB molecules. This weakened interaction manifested unfavorable

performances of AmB/U micelles, including poor stability, a rapid drug release and poor control on AmB aggregation. By mixing PEG-PUC and PEG-PBC in equimolar ratio, we were nonetheless able to achieve comparable antifungal activity to free AmB and Fungizone® without inducing nephrotoxicity. Through modulating the physical interactions between polymers and AmB, drug release and aggregation of AmB could be effectively controlled to improve toxicity without loss of efficacy. The rational design of AmB micellar formulations using biodegradable and functional polycarbonates is a potential strategy for improving the clinical treatment of systemic fungal infections.

Acknowledgments

The authors would like to acknowledge research funding and facilities provided by National University of Singapore (NUS) and Institute of Bioengineering and Nanotechnology (Biomedical Research Council and SERC Personal Care Program, Agency for Science, Technology and Research, Singapore). This research is supported by the Singapore Ministry of Health's National Medical Research Council under its Individual Research Grant Scheme (NMRC/1298/2011) awarded to P.R. Ee and Y.Y. Yang, the Ministry of Education Academic Research Fund (R148000200112) awarded to P.R. Ee, President's Graduate Fellowship to Y. Wang and J. S. Khara, NGS scholarship to X. Ke, SINGA scholarship to S. A. O. Obuobi, and A*STAR AGS scholarship to Z. X. Voo.

Reference

[1] S. Ravikumar, M.S. Win, L.Y. Chai, Optimizing outcomes in immunocompromised hosts: understanding the role of immunotherapy in invasive fungal diseases, Front. Microbiol. 6 (2015) 1322.
[2] A. Halperin, Y. Shadkchan, E. Pisarevsky, A.M. Szpilman, H. Sandovsky, N. Osherov, I. Benhar, Novel water-soluble amphotericin B-PEG conjugates with low toxicity and potent in vivo efficacy, J. Med. Chem. 59 (2016) 1197–1206.
[3] D.M. Casa, T.C. Carraro, L.E. de Camargo, L.F. Dalmolin, N.M. Khalil, R.M. Mainardes, Poly(L-lactide) nanoparticles reduce amphotericin B cytotoxicity and maintain its in vitro antifungal activity, J. Nanosci. Nanotechnol. 15 (2015) 848–854.
[4] J. Bolard, V. Joly, P. Yeni, Mechanism of action of amphotericin B at the cellular level. Its modulation by delivery systems, J. Liposome Res. 3 (1993) 409–427.
[5] D.M. Casa, T.K. Karam, C. Alves Ade, A.A. Zgoda, N.M. Khalil, R.M. Mainardes. Bovine serum albumin nanoparticles containing amphotericin B: characterization, cytotoxicity and in vitro antifungal evaluation, J. Nanosci. Nanotechnol. 15 (2015) 10183–10188.
[6] G. Barratt, S. Bretagne, Optimizing efficacy of amphotericin B through nanomodification, Int. J. Nanomed. 2 (2007) 301–313.
[7] R. Laniado-Laborin, M.N. Cabrales-Vargas, Amphotericin B: side effects and toxicity, Rev. Iberoam. Micol. 26 (2009) 223–227.
[8] K. Gilani, E. Moazeni, T. Ramezanli, M. Amini, M.R. Fazeli, H. Jamalifar, Development of respirable nanomicelle carriers for delivery of amphotericin B by jet nebulization, J. Pharm. Sci. 100 (2011) 252–259.
[9] J.J. Torrado, R. Espada, M.P. Ballesteros, S. Torrado-Santiago, Amphotericin B formulations and drug targeting, J. Pharm. Sci. 97 (2008) 2405–2425.
[10] M.S. Espuelas, P. Legrand, M.A. Campanero, M. Appel, M. Cheron, C. Gamazo, G. Barratt, J.M. Irache, Polymeric carriers for amphotericin B: in vitro activity, toxicity and therapeutic efficacy against systemic candidiasis in neutropenic mice, J. Antimicrob. Chemother. 52 (2003) 419–427.
[11] C. Yang, A.B. Attia, J.P. Tan, X. Ke, S. Gao, J.L. Hedrick, Y.Y. Yang, The role of non-covalent interactions in anticancer drug loading and kinetic stability of polymeric micelles, Biomaterials 33 (2012) 2971–2979.
[12] A. Lavasanifar, J. Samuel, S. Sattari, G.S. Kwon, Block copolymer micelles for the encapsulation and delivery of amphotericin B, Pharm. Res. 19 (2002) 418–422.
[13] I.L. Diaz, C. Parra, M. Linarez, L.D. Perez, Design of micelle nanocontainers based on PDMAEMA-b-PCL-b-PDMAEMA triblock copolymers for the encapsulation of amphotericin B, AAPS PharmSciTech 16 (2015) 1069–1078.
[14] C.H. Wang, W.T. Wang, G.H. Hsiue, Development of polyion complex micelles for encapsulating and delivering amphotericin B, Biomaterials 30 (2009) 3352–3358.
[15] M. Onda, Y. Inoue, M. Kawabata, T. Mita, Susceptibilities of phospholipid vesicles containing different sterols to amphotericin B-loaded lysophosphatidylcholine micelles, J. Biochem. 134 (2003) 121–128.
[16] M.L. Adams, G.S. Kwon, Relative aggregation state and hemolytic activity of amphotericin B encapsulated by poly(ethylene oxide)-block-poly(N-hexyl-L-aspartamide)-acyl conjugate micelles: effects of acyl chain length, J. Control Release 87 (2003) 23–32.
[17] A.C. Engler, X.Y. Ke, S.J. Gao, J.M.W. Chan, D.J. Coady, R.J. Ono, R. Lubbers, A. Nelson, Y.Y. Yang, J.L. Hedrick, Hydrophilic polycarbonates: promising degradable alternatives to poly(ethylene glycol)-based stealth materials, Macromolecules 48 (2015) 1673–1678.
[18] B. Wang, L. Chen, Y. Sun, Y. Zhu, Z. Sun, T. An, Y. Li, Y. Lin, D. Fan, Q. Wang, Development of phenylboronic acid-functionalized nanoparticles for emodin delivery, J. Mater. Chem. B Mater. Biol. Med. 3 (2015) 3840–3847.
[19] X.Y. Ke, V.W.L. Ng, S.J. Gao, Y.W. Tong, J.L. Hedrick, Y.Y. Yang, Co-delivery of thioridazine and doxorubicin using polymeric micelles for targeting both cancer cells and cancer stem cells, Biomaterials 35 (2014) 1096–1108.
[20] A.B. Attia, C. Yang, J.P. Tan, S. Gao, D.F. Williams, J.L. Hedrick, Y.Y. Yang, The effect of kinetic stability on biodistribution and anti-tumor efficacy of drug-loaded biodegradable polymeric micelles, Biomaterials 34 (2013) 3132–3140.
[21] P. Balabathula, D.R. Janagam, N.K. Mittal, B. Mandal, L.A. Thoma, G.C. Wood, Rapid quantitative evaluation of amphotericin B in human plasma, by validated HPLC method, J. Bioequiv. Availab. 5 (2013) 121–124.
[22] V.W. Ng, X. Ke, A.L. Lee, J.L. Hedrick, Y.Y Yang. Synergistic co-delivery of membrane-disrupting polymers with commercial antibiotics against highly opportunistic bacteria, Adv. Mater. 25 (2013) 6730–6736.
[23] M.M. Vila, S.L. Coelho, M.V. Chaud, M. Tubino, J.M. Jr, Oliveira, V.M. Balcao. Development and characterization of a hydrogel containing nitrofurazone for antimicrobial topical applications, Curr. Pharm. Biotechnol. 15 (2014) 182–190.
[24] Y. Wang, X.Y. Ke, J.S. Khara, P. Bahety, S. Liu, S.V. Seow, Y.Y. Yang, P.L. Ee, Synthetic modifications of the immunomodulating peptide thymopentin to confer anti-mycobacterial activity, Biomaterials 35 (2014) 3102–3109.
[25] J. Mishra, A. Dey, N. Singh, R. Somvanshi, S. Singh, Evaluation of toxicity & therapeutic efficacy of a new liposomal formulation of amphotericin B in a mouse model, Indian J. Med. Res. 137 (2013) 767–776.
[26] S.D. Li, L. Huang, Pharmacokinetics and biodistribution of nanoparticles, Mol. Pharm. 5 (2008) 496–504.
[27] T.S. Levchenko, R. Rammohan, A.N. Lukyanov, K.R. Whiteman, V.P. Torchilin, Liposome clearance in mice: the effect of a separate and combined presence of surface charge and polymer coating, Int. J. Pharm. 240 (2002) 95–102.
[28] S.H. Kim, J.P. Tan, F. Nederberg, K. Fukushima, J. Colson, C. Yang, A. Nelson, Y.Y. Yang, J.L. Hedrick, Hydrogen bonding-enhanced micelle assemblies for drug delivery, Biomaterials 31 (2010) 8063–8071.
[29] R.M. Versteegen, R.P. Sijbesma, E.W. Meijer, Synthesis and characterization of segmented copoly(ether urea)s with uniform hard segments, Macromolecules 38 (2005) 3176–3184.
[30] I. Gruda, N. Dussault, Effect of the aggregation state of amphotericin B on its interaction with ergosterol, Biochem. Cell. Biol. 66 (1988) 177–183.
[31] M.L. Adams, D.R. Andes, G.S. Kwon, Amphotericin B encapsulated in micelles based on poly(ethylene oxide)-block-poly(L-amino acid) derivatives exerts reduced in vitro hemolysis but maintains potent in vivo antifungal activity, Biomacromolecules 4 (2003) 750–757.
[32] R. Vakil, G.S. Kwon, Effect of cholesterol on the release of amphotericin B from PEG-phospholipid micelles, Mol. Pharm. 5 (2008) 98–104.
[33] T.A. Diezi, G. Kwon, Amphotericin B/sterol co-loaded PEG-phospholipid micelles: effects of sterols on aggregation state and hemolytic activity of amphotericin B, Pharm. Res. 29 (2012) 1737–1744.
[34] C. Yang, S.Q. Liu, S. Venkataraman, S.J. Gao, X. Ke, X.T. Chia, J.L. Hedrick, Y.Y. Yang, Structure-directing star-shaped block copolymers: supramolecular vesicles for the delivery of anticancer drugs, J. Control Release 208 (2015) 93–105.